FIV2024
IGUAÇU FALLS, BRAZIL
2-5 JULY 2024

FIV2024: FSI² & FIV + N
10th International Symposium on Fluid-Structure Interactions,
Flow-Sound Interactions, Flow-Induced Vibration & Noise

FIV2024-0128
Drag forces reductions in wake flow with flexible foils

Juan D'Adamo
Laboratorio de Fluidodinámica, Universidad de Buenos Aires - CONICET, Argentina
Instituto Franco-Argentino de Dinámica de Fluidos para el Medio Ambiente, IRL 2027, CNRS, UBA, CONICET, CABA, Buenos Aires, Argentina.
jdadamo@fi.uba.ar

Ramiro Godoy-Diana
Physique et Mécanique des Milieux Hétérogènes, ESPCI Paris-PSL (PMMH, UMR 7636), France
ramiro@pmmh.espci.fr

Abstract. *Drag forces in wake flow contribute to a large part of energy consumption in many industrial applications, particularly on transport. Strategies in flow control need solid knowledge on the physical mechanisms that characterizes wake flows. On one hand, active control involve the introduction of energy (e.g. mobile parts, blowing, suction, etc.) in a flow while passive control introduce modifications by changing the geometry, material, surface termination, etc. Wake flows are generally describes by the well known Bénard-Von Kármán (BvK) instability, an alternate vortex street pattern. To alter the flow pattern, a special configuration of flexible foils added to the surface of a bluff body is tested and can result in significant drag reductions. These are due to reconfiguration, see Gosselin* et al. *(2010), and modification of the hydrodynamical stability properties (Strykowski and Sreenivasan, 1990; Giannetti and Luchini, 2007; Thiria* et al.*, 2009). On a recent work, García-Baena* et al. *(2021) obtained drag reductions that can be applied to a better aerodynamical design of trucks. In the present work, we study the strong fluid structure interaction experimentally in wind tunnels for a D-shape body. We characterize the modifications on the BvK vortex street by reconfiguration and vibrations of the foils induced by the wake. The results will help develop efficient aerodynamic designs to ultimately reduce energy consumption.*

Keywords: *Wake Flows, Aeroelasticity, Drag Reduction*

1. INTRODUCTION

The flow around a circular cylinder is a practical benchmark to study bluff body wakes. Through this problem, important applications concern engineering and environmental sciences. The Reynolds number $Re = u_\infty D/\nu$ defines the different flow regimes that takes place. A stationary state in the wake $5 < Re < 47$ is characterized by the linear growing of two well defined eddies of opposite recirculation. After $Re > 47$, following an inviscid instability, the eddies shed alternatively forming the Bénard-Von Kármán vortex street (BvK). Its frequency f_{vs} is made non dimensional by the Strouhal number $St = f_{vs}d/u_\infty$, which evolves in the range $[0.11, 0.2]$. Even if the flow experiences three dimensional destabilization ($Re \sim 180$) BvK structures remain for a long range of Re numbers.

Drag forces are strongly related to the wake dynamics, and by means of flow control, they can be modified. Hence, efficient flow control strategies for the cylinder wake involve the manipulation of BvK structures in order to reduce drag forces. On one hand, active control add energy to the flow from an external devices such as mechanical movement of the cylinder (Thiria *et al.* (2006)), introducing moving flaps (Bao and J., 2013) blowing or suction in the surface (Kim and Choi, 2005), MEMs or electrohydrodynamic actuators (Jukes and Choi (2009); D'Adamo *et al.* (2017)). Important reductions of drag forces are thus obtained with energy savings. On the other hand, passive control implies no external addition of energy, so the shape of the bluff body can be modified. A dimpled surface of the cylinder (Bearman and Harvey, 1993) can reduce drag by advancing the critical Reynolds number, which is for a smooth cylinder about $3 \cdot 10^5$, to $6 \cdot 10^4$. Also, an early device to control vortex shedding is the splitter plate by Roshko (1955). To reduce drag forces, the numeric simulation of Yoon *et al.* (2014) proposed two plates behind the cylinder that interact with vortex production. In the same sense, Wu *et al.* (2016) performed the study of two flexible filaments of fixed length, with varying position behind the cylinder. They achieved important drag coefficient reduction for the case of flapping filaments at frequencies related to the natural vortex shedding. On a recent work, based on a similar configuration, García-Baena *et al.* (2021) obtained drag reductions that can be applied to a better aerodynamical design of trucks. It is also worth mentioning the work by Gosselin *et al.* (2010) that studied how flexible plates reconfiguration can achieve

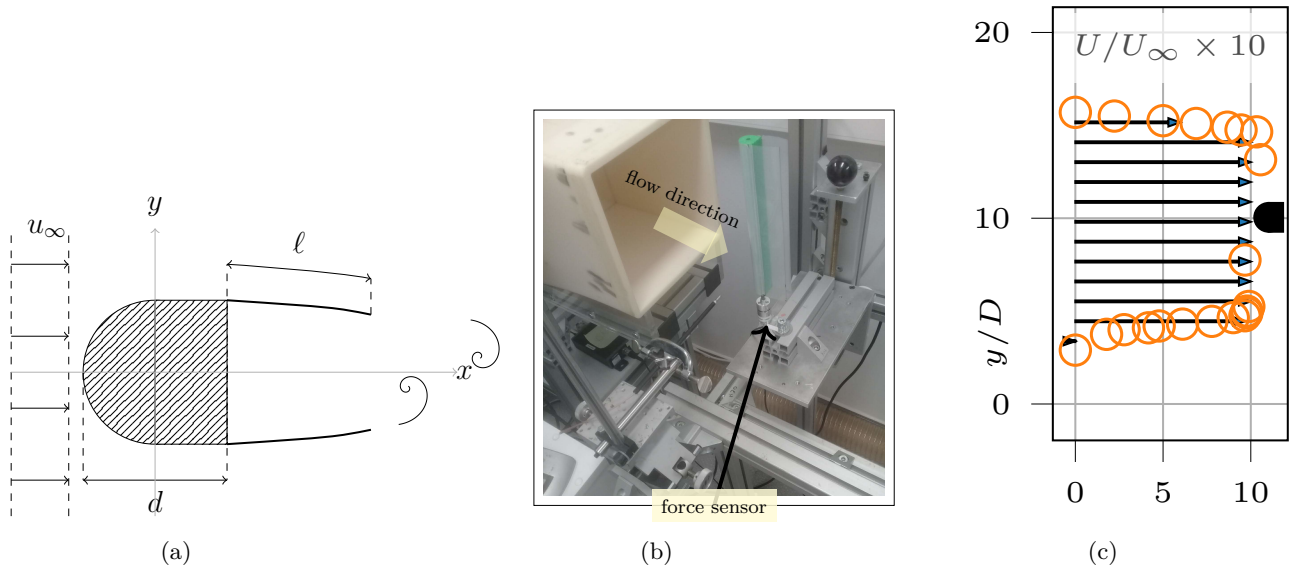

(a) (b) (c)

Figure 1: a) Scheme of the flow configuration around a D-shaped cylinder. b) Photography of the device at the cross section of an open Wind Tunnel. c) Wind tunnel velocity flow profile.

important drag reductions in wakes and how non dimensional parameters can lead to the construction of a simple model.

2. Experimental Setup

In the present work, we tested the ability of flexible flaps to reduce drag forces on a D-shaped cylinder as shown in Figure 1a. The experiments were conducted in an open wind tunnel of the PMMH Laboratory, Figure 1b. The test section of this facility is of $0.20 \times 0.20\,\mathrm{m}^2$, a total length of 1.80 m and the flow velocity during experiments was set from $u_\infty = 4$ to 13m/s.

Fig.1c) presents the velocity profile measured with a pitot probe in order to ensure a uniform flow across the cylinder.

The wake flow was generated with a smooth cylinder of external diameter $D = 20 \times 10^{-3} m$ and a spanwise length $h = 0.18m$. We have measured the drag exerted on the cylinder by means of a force sensor F/T Sensor: Nano17, that enable us to detect changes of 3 mN in the force.

The blockage ratio was 10%, no correction has been applied to the drag data for blockage effects. A set of flexible flaps made of polystyrene of different thicknesses was attached to the cylinder at $\theta = 90°$ measured from the stagnation point as illustrated in Fig. 1a. The flap lengths ℓ were $\ell/D \in [0.75, 1.00, 1.25, 1.5]$ in order to explore the strong coupling between the flow and the elastic response of the material. Flexural rigidities were obtained using the bending test suggested by Stuart (1966), being the resulting values ($B = [0.45, 5.58, 45.1]10^{-5}\mathrm{N\,m}$).

Let's mention that for the range of measured Reynolds numbers, $St \simeq 0.2$ and we can have a reasonable estimation of f_{vs}. For the velocity range, using D as characteristic length it means $f_{vs} \in [40 \ldots 132]$Hz. On the other hand, the natural frequency of the flap can be estimated by considering it as a cantilever beam in free vibration. This means $\mu\ddot{w} + Bw^{iv} = 0$, where μ is the mass per unit length, w is the beam displacement, and B the flexural rigidity, so the natural frequencies are given by $f_s = 2\pi k_n^2 (B/\mu)^{1/2}$. For the first mode of vibration, $k_1\ell = 1.875$, so for the tested lengths and rigidities, the natural frequency goes $f_n \in [7, \ldots, 142]$. Therefore, hydrodynamic and elastic times are comparable as we expected by selecting the flap material and lengths.

Fast camera images were acquired in order to characterize the deformation and dynamics of the flaps, with a PHANTOM Miro C211 High-Speed Camera. Images of 1280×1090 px^2 were acquired at 1800 frames per second. A photography of the D-shape body with the flaps is presented in Figure 2a. A set of 2000 images was processed with Fourier analysis in order to get their dynamics.

We measure vortex shedding frequencies with a Dantec CTA Hot Wire Anemomoter, at a sampling rate of 1000 Hz. With a probe placed at symmetry $y = 0$ and downstream distances $x \in [1, \ldots, 2]D$ we measured the velocity fluctuations and calculate the flow global frequency as showed on Fig. 2b. When flaps move with the flow, we retrieve the same flow frequency from the series of images signal processing on Fig. 2c. In addition,

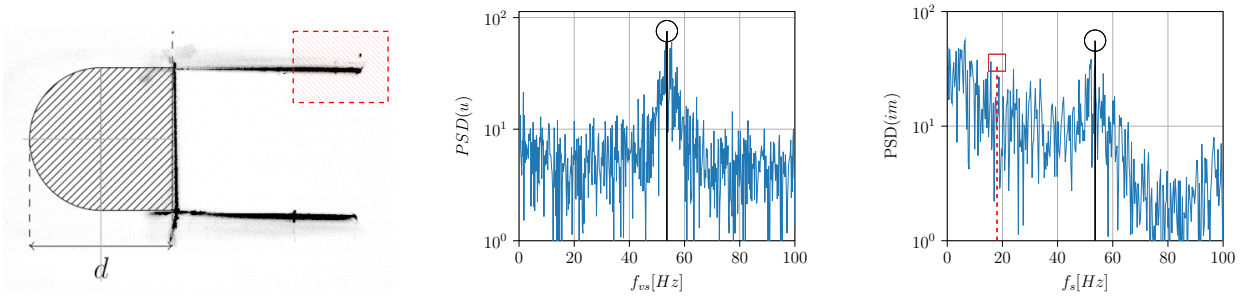

(a) (b) (c)

Figure 2: Data from fast Camera and Hotwire anemometer for parameters $u_\infty = 4.66\,\mathrm{m/s}$, $\ell = 1.50D$, $B = 5.58{\cdot}10^{-5}\mathrm{N\,m}$. (a) Photography of the flaps in combination with the body scheme. The hatched area around the flaps in the image is used as input for Fourier analysis. (b) Typical output for the spectrum of the hotwire signal located in the wake. Maximum at 53.6 Hz corresponds to a Strouhal number of 0.23. (c) Processing output for a series of camera images, as indicated in (a). Flow (◯) and first mode elastic vibrations (□) frequencies are present.

other frequencies are also present, related to first mode of elastic vibration $f_s = 2\pi k_1^2 (B/\mu)^{1/2}$. Recalling that $k_1\ell = 1.875$, the corresponding theoretical value is 18.03 Hz which is plotted in a red dashed line on the Figure. The spectrum presents a peak at 16 Hz which is not far from the theoretical value. There are also other peaks that can be identified as a combination of both frecuencies,vortex shedding f_{vs} and solid elastic vibrations f_s through nonlinear effects.

3. Results and Discussion

A first attempt to characterize the flow control performance was to measure drag forces for each rigidity B varying flap lengths for a range of Reynolds numbers, as shown in Figure 3. The reference drag coefficient for the D-shape was almost constant, independent of the Reynolds number, $C_{D0} = 0.87$. The most flexible case, Fig. 3a, shows reductions for all lengths, which are slightly more pronounced for $\ell/D = 1.50$. From $C_D = 0.6$ at $\mathrm{Re} = 5000$, the drag coefficient reduces monotonically to obtained a minimum value of $C_D = 0.48 = 0.55C_{D0}$ at $\mathrm{Re} \simeq 10000$. This is also a threshold as a sudden increase of drag is observed, until it reaches the non-controlled values, C_{D0}. This is observed for any length and is caused by the material becoming completely folded. The momentum of the flow is large enough to overcome the elastic resistance of the flap. We can compare it through a version of Cauchy non-dimensional number

$$\tilde{\mathrm{Ca}} = \frac{\rho u_\infty^2 \ell D h}{B} \tag{1}$$

In this way, we are able to compare the torque produced from the load caused by the free flow on the flaps and their corresponding flexural rigidities.

In the following case (see Fig. 3b), the rigidity is higher, and although there is deformation, it does not reach such dramatic values as to be fully folded. The minimum values, of about $0.35C_{D0}$ are obtained for the larger lengths $\ell/D = 1.25$ and 1.50 and $\mathrm{Re} \leq 8000$.

Finally, in the most rigid case shown in Fig. 3c, drag reduction values corresponding to shorter lengths $\ell/D = 0.75$ and 1.00 reach $C_D \simeq 0.5$. The minimum drag also corresponds to lengths $\ell/D = 1.25$ and 1.50. The influence of Reynolds numbers is almost negligible.

We present an initial explanation of the behavior of a bluff body combined with flexible flaps. On one hand, it is widely recognized that increasing the aspect ratio of a rectangular cylinder leads to drag reductions (Bearman and Trueman (1972)). On the other hand, as the flaps are deformed under the flow momentum, we expect the forces will decrease accordingly. Figure 4 presents the ratio between the drag for each case compared to the reference C_D/C_{D0} plotted against the Cauchy number defined in equation (1). All data are represented as each length ℓ/D and stiffness B of the material. From $\tilde{\mathrm{Ca}}$ numbers, we can distinguish three regimes: 10^2, the most rigid case, presents drag reductions up to 50%; 10^4 the most flexible case, achieves moderate reductions until the flaps become fully folded and lose control effectiveness; 500 where strongest drag reductions are obtained for lengths $\ell/D = 1.25$ and 1.50. We observe a significant discontinuity of drag values at $\tilde{\mathrm{Ca}} \sim 200$ and it can be explained in terms of the dynamics of the flaps: when the flexural rigidity is $B = 45.1 \times 10^{-5}\,\mathrm{N\,m}$, the motion is very weak. While Cauchy numbers are almost the same for i.e. $\ell/D = 1.50$ and $B = 5.58 \times 10^{-5}\,\mathrm{N\,m}$, the associated elastic frequency is quite different as is showed on Figure 5.

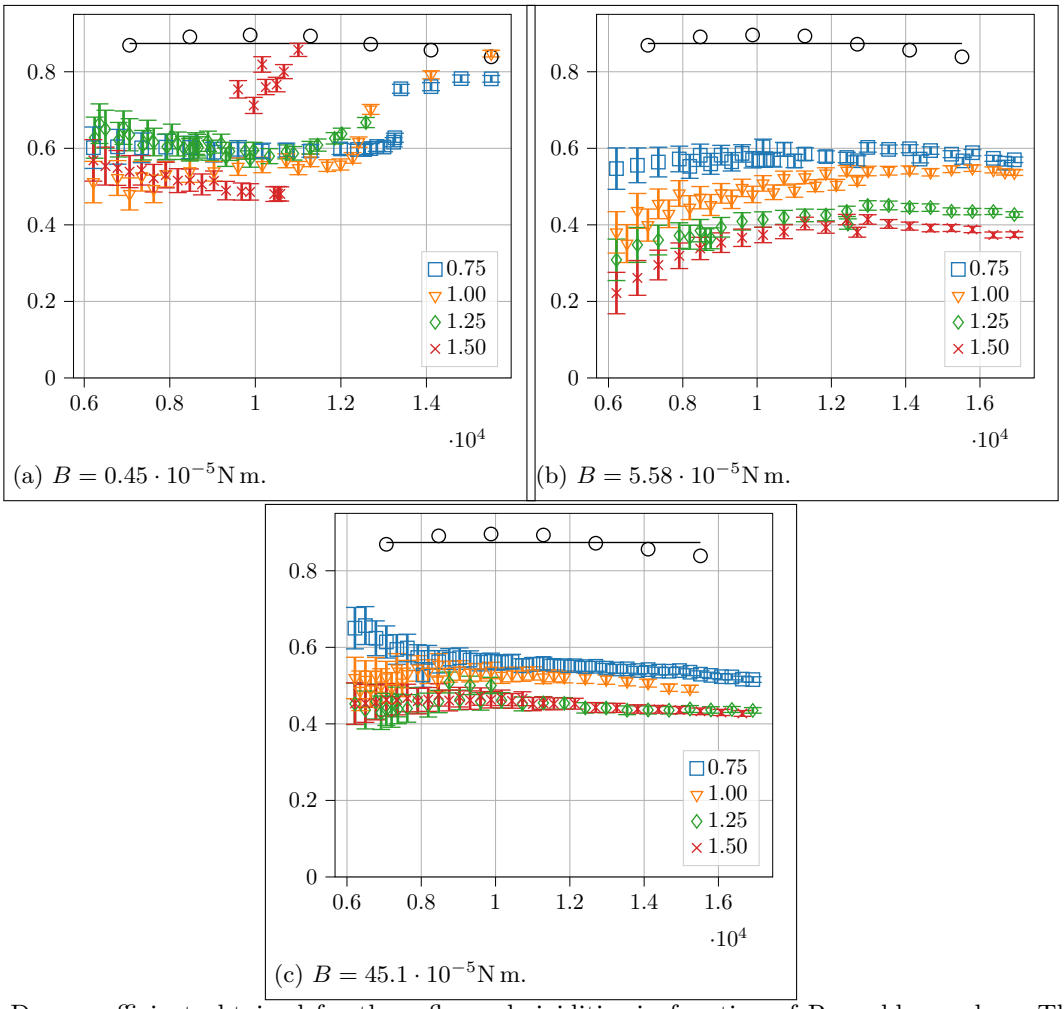

Figure 3: Drag coefficient obtained for three flexural rigidities in function of Reynolds number. The varyng parameter for each plot is the length of the flexible flaps ℓ/D attached to the D-shaped cylinder.

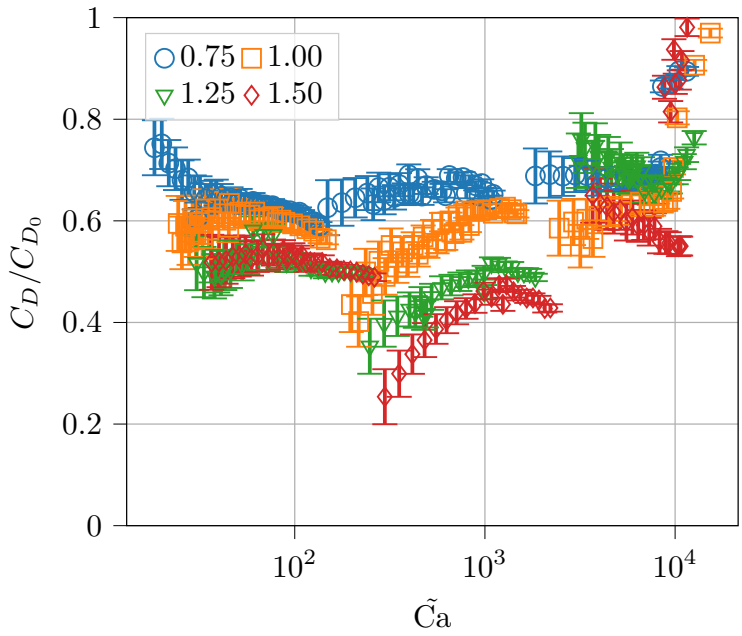

Figure 4: Normalized drag and Cauchy number. Three working regimes are distinguished: the most rigid, low $\tilde{Ca}$ presents slight deformations; the middle shows deformation and also vibration to produce the highest drag reductions; high $\tilde{Ca}$ means too much flexibility that can lead to the complete folding of the flaps.

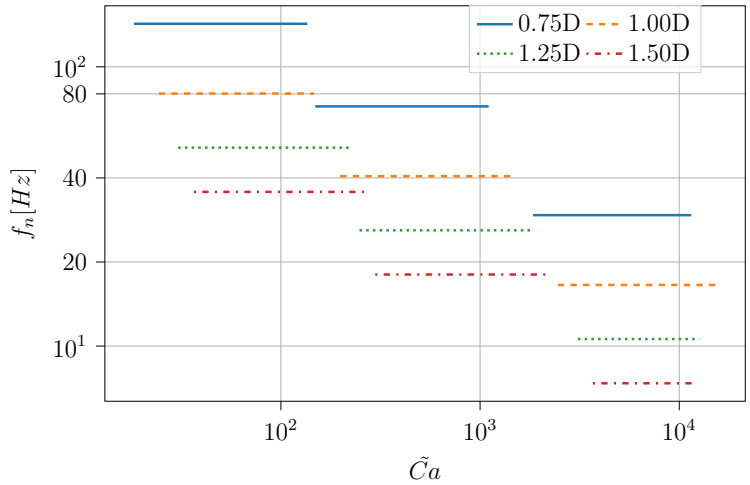

Figure 5: Theoretical natural frequency for the first mode of vibration.

Therefore, we can conclude that passive control effectiveness is not only influenced by bluff body aspect ratio and profiling through reconfiguration, but also by the flaps vibration. The highest drag reductions are produced by low frequency ratios, specifically $f^+ = f_n/f_{vs} < 1/3$. One potential explanation for this phenomenon is that a burst-coast-like flow control mechanism may be triggered as the flaps move. Further studies on velocity flow fields could complement these findings.

ACKNOWLEDGEMENTS

This work was funded by the International Research Laboratory (IRL) between France and Argentina: Institut Franco-Argentin de Dynamique des Fluides pour l'Environnement (IFADyFE).

REFERENCES

Bao, Y. and J., T., 2013. "Active control of a cylinder wake flow by using a streamwise oscillating foil". *Physics of Fluids*.

Bearman, P. and Harvey, J., 1993. "Control of circular cylinder flow by the use of dimples". *AIAA journal*, Vol. 31, No. 10, pp. 1753–1756.

Bearman, P. and Trueman, D., 1972. "An investigation of the flow around rectangular cylinders". *Aeronautical Quarterly*, Vol. 23, No. 3, pp. 229–237.

D'Adamo, J., Leonardo, L., Castro Hebrero, F., Sosa, R., Duriez, T. and Artana, 2017. "Circular cylinder drag reduction by three-electrode plasma symmetric forcing". *ASME J. Fluids Eng.*

García-Baena, C., Jiménez-González, J. and Martínez-Bazán, C., 2021. "Drag reduction of a blunt body through reconfiguration of rear flexible plates". *Physics of Fluids*, Vol. 33, No. 4, p. 045102.

Giannetti, F. and Luchini, P., 2007. "Structural sensitivity of the first instability of the cylinder wake". *Journal of Fluid Mechanics*, Vol. 581, pp. 167–197.

Gosselin, F., De Langre, E. and Machado-Almeida, B.A., 2010. "Drag reduction of flexible plates by reconfiguration". *Journal of Fluid Mechanics*, Vol. 650, pp. 319–341.

Jukes, T.N. and Choi, K.S., 2009. "Long lasting modifications to vortex shedding using a short plasma excitation". *Phys. Rev. Lett.*, Vol. 102, p. 254501.

Kim, J. and Choi, H., 2005. "Distributed forcing of flow over a circular cylinder". *Physics of Fluids*, Vol. 17, No. 3, p. 033103.

Roshko, A., 1955. "On the wake and drag of bluff bodies". *Journal of the Aeronautical Sciences (AIAA)*, Vol. 22, No. 124.

Strykowski, P. and Sreenivasan, K., 1990. "On the formation and suppression of vortex 'shedding'at low reynolds numbers". *Journal of Fluid Mechanics*, Vol. 218, pp. 71–107.

Stuart, I., 1966. "A loop test for bending length and rigidity". *British Journal of Applied Physics*, Vol. 17, No. 9, p. 1215.

Thiria, B., Goujon-Durand, S. and Wesfreid, J.E., 2006. "Wake of a cylinder performing rotary oscillations". *Journal of Fluid Mechanics.*, Vol. 560, pp. 123–147.

Thiria, B., Cadot, O. and Beaudoin, J.F., 2009. "Passive drag control of a blunt trailing edge cylinder". *Journal of fluids and structures*, Vol. 25, No. 5, pp. 766–776.

Wu, J., Wu, J. and Zhan, J., 2016. "Characteristics of flow over a circular cylinder with two attached filaments". *Journal of Fluids and Structures*, Vol. 66, pp. 269–281.

Yoon, J., Kim, J. and Choi, H., 2014. "Control of laminar vortex shedding behind a circular cylinder using tabs". *Journal of Mechanical Science and Technology*, Vol. 28, No. 5, pp. 1721–1725.